Malaysian Journal of Chemistry, 2015, Vol. 17(1), 1–11

Properties of Iron Oxide Nanoparticles

H. T. Ong, M. J. Nurhidayatullaili*, B. A. H. Sharifah, O. Boondamnoen and M. F. Tai

Nanotechnology and Catalysis Research Centre, Institute of Post-graduate Studies, University of Malaya, 50603 Kuala Lumpur, Malaysia

*Corresponding author (e-mail: nurhidayatullaili@um.edu.my)

Due to hygienic concerns in gloves are required to be worn in food, pharmaceutical processing and healthcare industries. In fact, these gloves might tear off and contaminate the food and pharmaceutical or healthcare products during the manufacturing and packaging process. The white or light flesh-coloured gloves are not easy to detect by naked eyes, subsequently they lead to difficulty in removal before shipping. In this paper, iron oxide nanoparticles were selected as additive for nitrile butadiene rubber in order to improve the detectability of gloves by mean of its magnetic properties. Iron oxide nanoparticles (IONs) were synthesized via precipitation method with monosalt iron (II) sulphate heptahydrate and ammonium hydroxide as precursors at 60°C. The properties of IONs were investigated by zetasizer, X-ray diffractometry (XRD), transmission electron microscopy (TEM), Raman spectroscopy and vibrating sample magnetometer. Based on zetasizer analysis, iron oxides were found in average hydrodynamic size 87.8 nm. By using Scherrer equation, XRD showed an average of 25.95 nm crystallite size. Semispherical shape with 15.4 nm of IONs were observed by TEM. Magnetite and maghemite phase were found in the range of 670 cm^{-1} and 700 cm^{-1} respectively, through Raman spectroscopy. Finally, IONs with 70.1 emu/g of magnetization saturation were able to form acrylonitrile butadiene rubber/IONs composite with 3.8 emu/g magnetization saturation.

Key words: Iron oxide nanoparticles; precipitation; magnetic properties; magnetization; maghemite; hematite; NBR latex film

Received: October 2014; Accepted: April 2015

Iron oxide nanoparticle (ION) has been widely used in various applications especially in food packaging. Due to its unique properties, researchers started to venture into other applications such as anti-vibration where magnetite-filled elastomer has been designed as active dampers [1]. Besides, magnetite-embedded thermo-sensitive polymer was synthesized to produce magnetic plastic materials. It tends to contract or swell dramatically when temperature is increased or magnetic field is applied [2]. Moreover, smart materials that consist of magnetic nanoparticles with an amphiphilic biocompatible polymer have great application such as artificial muscle, temperature and pH sensors, and micro-fluidic devices.In pharmaceutical and food processing industries, hygiene is of great concern and protective equipment such as gloves which are used to prevent any contaminant existing in the products. Having said that, glove tear is not avoidable because it is a thin and soft article and may come in contact with sharp objects. Thus, when iron oxide nanoparticle is incorporated into into acrylonitrile butadiene rubber (NBR), any torn fragment of the NBR glove left in the product could be detected by a metal detactor.

Properties of IONs are investigated due to sediment of magnetite phase which would affect the magnetization of final products. According to Vandenberghe *et al*. [3], nanosize magnetite tends to oxidise into maghemite or hematite due to their large surface area. Decreasing of magnetite in IONs tends to impact the magnetic properties [4]. Apart from that, crystallite sizes

diffractometer).

of IONs are investigated, as they will directly influence the magnetization as well. Berkowitz *et al*. [5] reported that magnetic properties are strongly affected by the crystallite size of IONs. Furthermore, particle size of IONs is investigated as it indirectly contributes to its magnetization. Hence, X-ray diffraction (XRD) is used to further investigate on its crystallite size, zetasizer for the particle size analysis, Raman spectroscopy for the IONs phase and vibrating sample magnetometer (VSM) for the magnetization saturation.

MATERIALS

All chemicals were purchased from Merck Millipore. Iron (II) sulphate heptahydrate ($FeSO_4.7H_2O$) was used as iron salt precursor. Ammonium hydroxide (NH_4OH, 25%) was used as base precursor. Ethanol 95% AR grade and deionised (DI) water were used to wash samples. NBR latex (acrylonitrile content: 24%–26%) was supplied by Synthomer Sdn. Bhd.

METHODOLOGY

Synthesis of IONs

$FeSO_4.7H_2O$ was mixed with 50 ml water to form 0.2 M iron salt precursor while NH_4OH, 25% was added to 50 ml water to form 6.68 M of base precursor. Iron salt precursor was stirred for 15 min and ultrasonicated for 10 min to produce a well dissolved $FeSO_4$. Iron salt precursor was poured once into base precursor, subsequently stirred for 1 h. Final solution was washed with DI water for 5 times and decanted by using neo magnet. The produced precipitate was dried at 50°C overnight.

Preparation of NBR/IONs Composite Film

IONs and NBR latex were mixed and stirred with 50 rpm for an hour at room temperature. 2 g of compounded latex were casted on a petri dish (area: 38.48 cm^2) in order to obtain a thin layer of latex. After that, it was cured in the oven at 80°C for 45 min and finally NBR/IONs composite films were formed.

Characterization of IONs

Crystallite phase of IONs was determined by X-ray diffraction using Cu Kα radiation (XRD, λ = 1.5406 Å, Bruker axs D8 Advance diffractometer). From the result, the crystalline size of magnetite nanoparticle could be determined by using Scherrer equation. Besides, Raman spetroscopy (Renishaw in Via Reflux with high performance CCD camera and LEILA microscope) were used in this study. Scattered radiation was collected by focusing laser beam via ×50 objective and the laser spot on sample was approximately 0.836 μm with 514 nm excitation. Argon gas laser (514 nm) was selected in our paper as 1800 mm^{-1} spectral due to its resolution is sufficient to plot a good spectra. Malvern zeta sizer was used to determine hydrodynamic size of IONs. Approximately 0.5 mg of IONs was weighed and dispersed in 5 ml of water. Two drops of 3 M ammonium hydroxide were added to the solution untila pH value of 9 to 10 was reached. In this condition, IONs were dispersed well and less agglomerated. High resolution transmission electron microscopy (TEM) analysis was performed by JEM-2100F instrument with accelerating voltage 200 kV. Samples were prepared by dropping dispersed IONs on copper grids of 300 mesh. The measurement of lattice-fringe spacing was carried out by using Image-J. Besides, 50 IONs particles were measured to determine particle size distribution. VSM (Lakeshore – VSM 7407) was used to study magnetic properties of IONs. Roughly 0.03 g of IONs was prepared and magnetic field from –12 500 G to 12 500 G was applied to identify magnetization saturation.

Characterization of NBR/IONs Composite

The magnetic properties of NBR/IONs composites were evaluated by VSM with the small piece (3 × 3 mm^2) of NBR/IONs composite film cutting. The sample was pasted at sample holder before starting to ramp up magnetic field from –10 000 G to 10 000 G.

RESULTS AND DISCUSSION

Figure 1 demonstrates XRD patterns of IONs. XRD patterns confirmed that magnetite and maghemite were formed at all the conditions applied. In fact, they were further confirmed by their composition of Fe_3O_4 and γ-Fe_2O_3 nanocrystal as their main peaks of the position and relative intensity were

matching well with JCPDS card (19-0629) and JCPDS card (39-1346), respectively. Unstable Fe^{2+} cations in inverse-spinel magnetite octahedral site were easily oxidised into Fe^{3+}. This is applied for both methods since open environment conditions have been used (room temperature and humidity) [8]. A range of partially oxidized magnetite to fully oxidized maghemite was formed. Scherrer equation was implemented to calculate crystallite size of IONs at corresponding peaks of (220), (311), (400), (422), (511) and (440) which is illustrated in Table 1. IONs with 42.4 nm crystallite size were determined at plane (311) and it was the highest peak shown in Figure 1. Average crystallite size, 25.95 nm was large and it contributed to greater magnetic properties of IONs. Demortiere *et al*. [6] reported that crystallite size was increased from 3.1 nm to 12.8 nm by XRD were increasing the magnetization saturation at –268°C from 29 to 77 emu/g. This is good agreement with Kim *et al*., who mentioned that particle size is linearly increased with crystallite size [7].

Figure 2 depicts a Raman spectrum of IONs where magnetite and maghemite are shown in different peaks. Li *et al*. [8] stated that magnetite

Table 1. XRD data for IONS at different planes.

Degree (2θ)	30.2	35.5	43.2	53.7	57.1	62.7	
Crystalline plane (hlk)	(220)	(311)	(400)	(422)	(511)	(440)	Average
Theory value of JCPDS card (19-0629)	0.297	0.253	0.210	0.171	0.162	0.148	0.207
Theory value of JCPDS card (39-1346)	0.295	0.252	0.209	0.170	0.161	0.148	0.206
Crystallite size of IONs (nm)	34.9	42.4	21.7	14.1	23.0	19.7	25.95

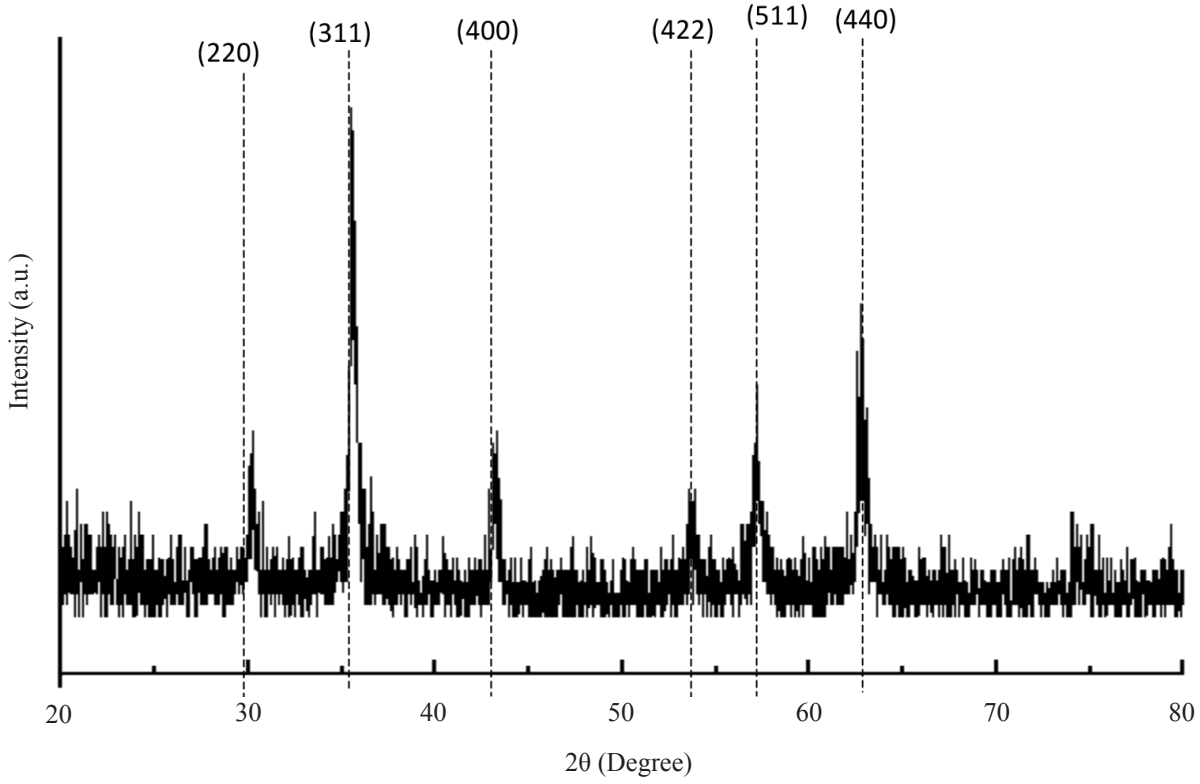

Figure 1. XRD pattern of IONs.

is a poor Raman scatterer because low laser power is needed (less than 0.35) to prevent phase transformation of magnetite to maghemite or further transform to geotite and hematitie. Thus, in this study 0.2 mV was selected in the Raman analysis but longer exposure of laser irradiation would still induce the transformation of magnetite. According to Slavov [9], magnetite has a strong peak at 668 cm^{-1} and maghemite has strong peaks at 350 cm^{-1}, 500 cm^{-1} and 700 cm^{-1} while hematite has strong peaks at 225 cm^{-1}, 299 cm^{-1} and 412 cm^{-1}. From Figure 2, there is no obvious peak of hematite recorded. This could be explained by the oxidation rate of Fe^{2+} which depended on the presence of inorganic ligands. Oxidation rate decreased from perchloride, fluoride, nitrate, chloride, carbonate, sulphate, silicate until phosphate [10]. It was expected that a slow oxidation rate might prevent further transformation of maghemite to hematite.

Zeta potential has been used to determine the surface charge of IONs. It has been recorded that, the zeta potential of IONs was –48.2 mV which was covered by the negative surface charge on their surface. According to Sun *et al*. [11], iso-electric point (IEP) of IONs was near pH 8.3. IEP is the critical pH value whereby the net surface charge is zero. The solution of IONs was adjusted to pH 9 – 10 which exceeded the critical pH of 8.3. Thus, it was confirmed that, the produced IONs were highly stable within pH 9–10. This was due to the repulsive force between IONs particles. Besides, metastable suspension of IONs can be achieved when the zeta potential is less than –30 mV [12]. Hence, the pH range of 9 – 10 led to a high colloidal stability of IONs in water and they were further suitable to be incorporated with NBR latex. Hydrodynamic size of IONs was 87.8 nm which was still considered as nanosize. Figure 3 shows hydrodynamic size distribution of IONs and it gives a polydispersity index of 0.114. Since its polydispersity is lower than 0.2, it can be considered as monodispersed [13]. The highest volume percentage size was 78.8 nm meanwhile the lowest volume percentage size was 295.3 nm. Haryono *et al*. [14] reported that IONs produced was 2.1 ± 0.9 nm with polydispersity

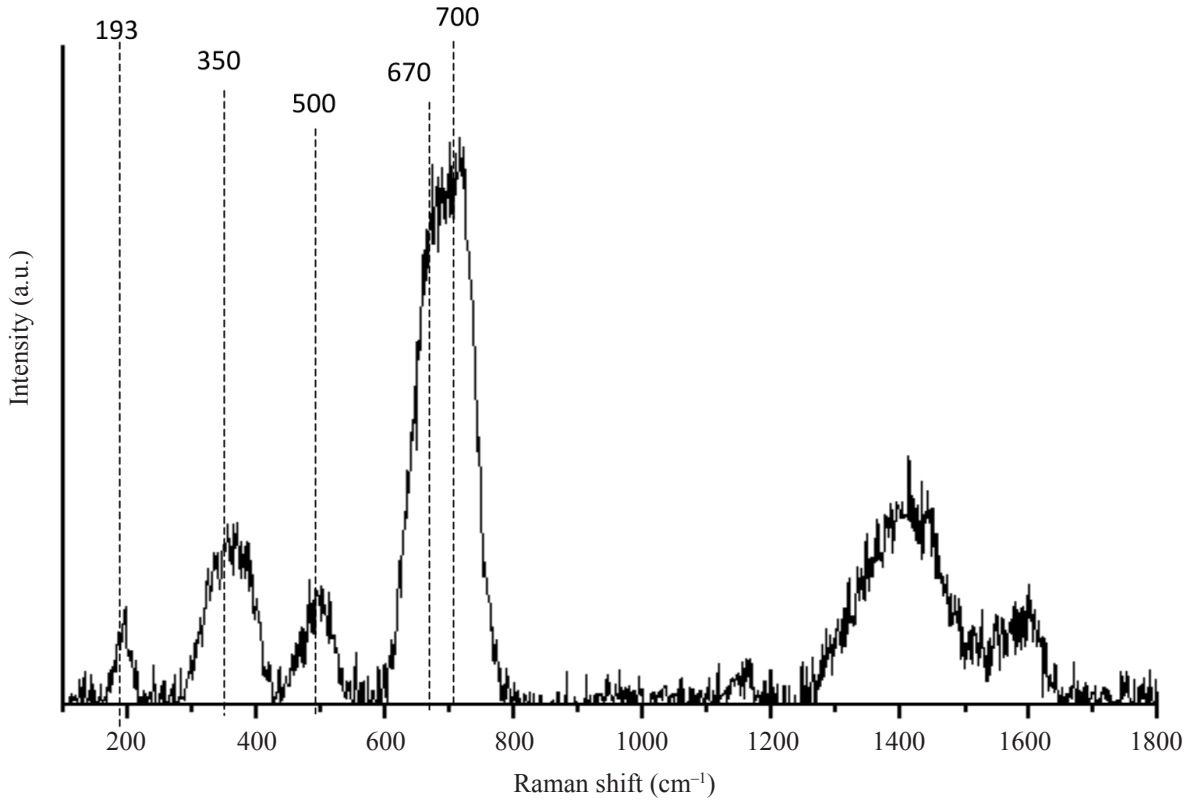

Figure 2. Raman spectra of IONs.

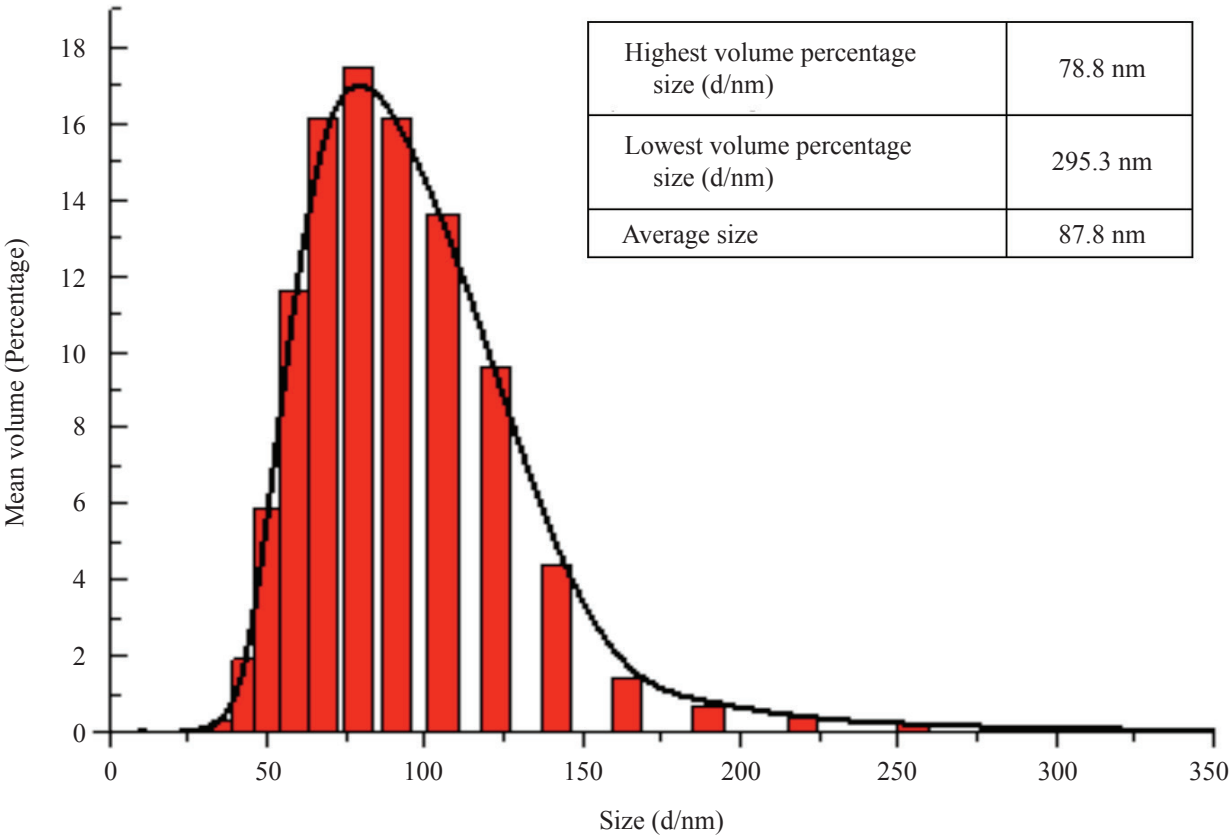

Figure 3. Hydrodynamic size distribution of IONs.

index of 0.327. Even though our IONs size was larger, it showed narrow sized distribution. Higher monodisperse IONs led to uniform magnetic properties distribution on NBR latex.

High-resolution TEM (HRTEM) analysis of IONs with 50 000 times magnification and 100 000 times magnification are shown in Figures 4a and 4c, respectively. In general, the IONs particles are demonstrated in semispherical shapes with an average size of 15.2 nm (Figure 4). The most particle size is in the range of 18 nm to 20 nm and it is close to average crystallite size 25.95 nm (Table 1). Particle size and crystallite size are correlated to each other, thus influencing the magnetic properties of IONs [7]. Agglomerated IONs can be seen clearly in Figure 4a and 4c. This is due to the nature of IONs which consist of van der Waals forces and magnetic dipolar forces among the particles. Van der Waals forces result in short range isotropic attraction whilst magnetic dipolar forces induce anisotropic interactions between the IONs particles [15]. It could be expected that, surface modification and coating of IONs be carried out to minimize the agglomeration while improving compatibility of IONs to NBR latex. Figure 4d shows a typical HRTEM image of IONs with 22.3 nm of size. These nanosize IONs were found in the sample with interplanar distances of d_1 = 0.292 nm, d_2 = 0.3 nm and d_3 = 0.259 nm that were very close to planes (220) and (311) as shown in Table 1. Thus, it further confirms that $Fe_3O_4$and γ-Fe_2O_3 exists in the sample [16].

Figure 5 shows ferromagnetic hysteresis loop of IONs. In general, Ms of bulk magnetite is recorded at 92 emu/g. However, the produced IONs have lower Ms which is 70.1 emu/g at 12500 G [17]. Magnetic properties of IONs are considered quite strong because of its large diameter of crystallite size. IONs indicate small coercivity at ±100 G and remanence at ±10 emu/g. According to Zhang *et al*. [18], zero remanence and coercivity represent the superparamagnetic

(a)

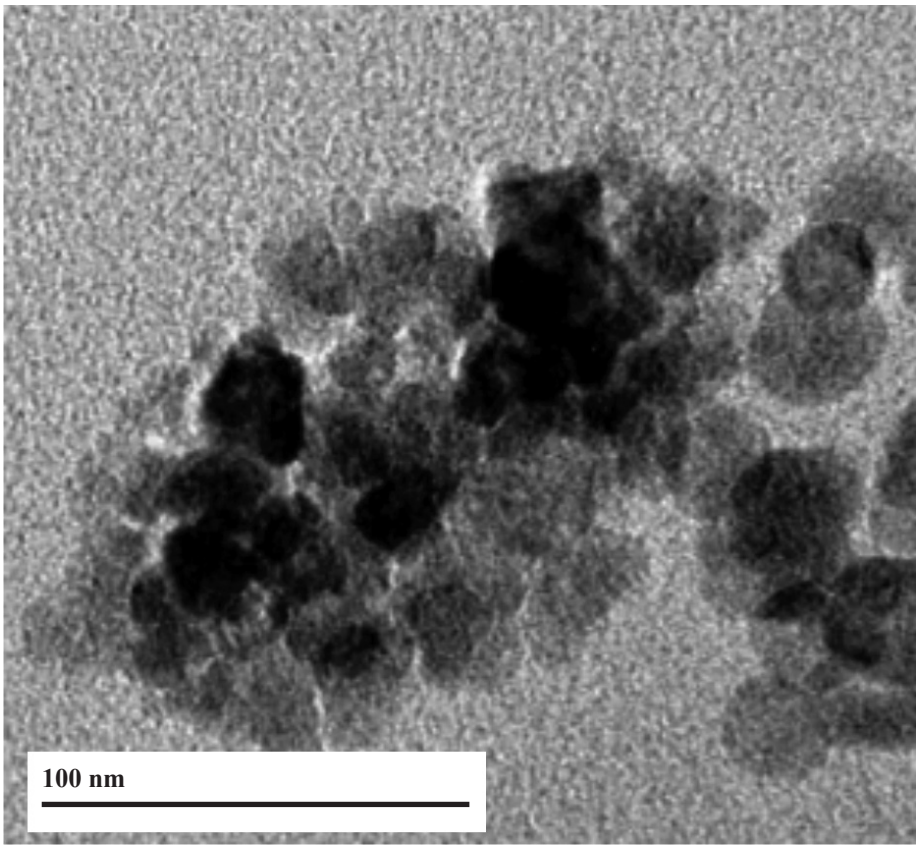
100 nm

(b)

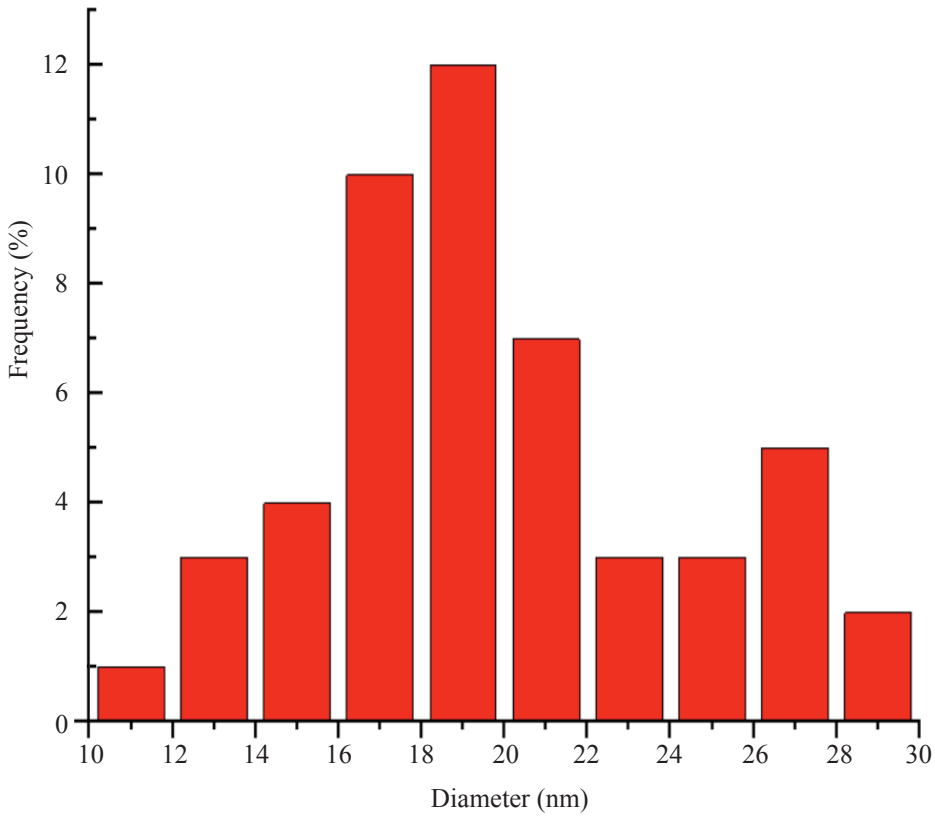
Frequency (%)
0
2
4
6
8
10
12
10
12
14
16
18
20
22
24
26
28
30
Diameter (nm)

(c)

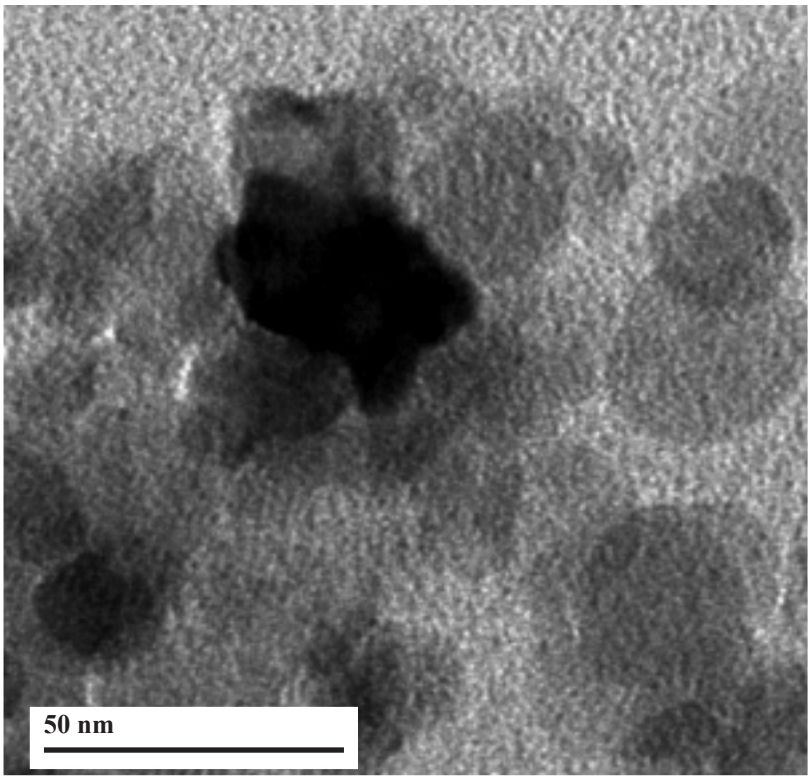

(d)

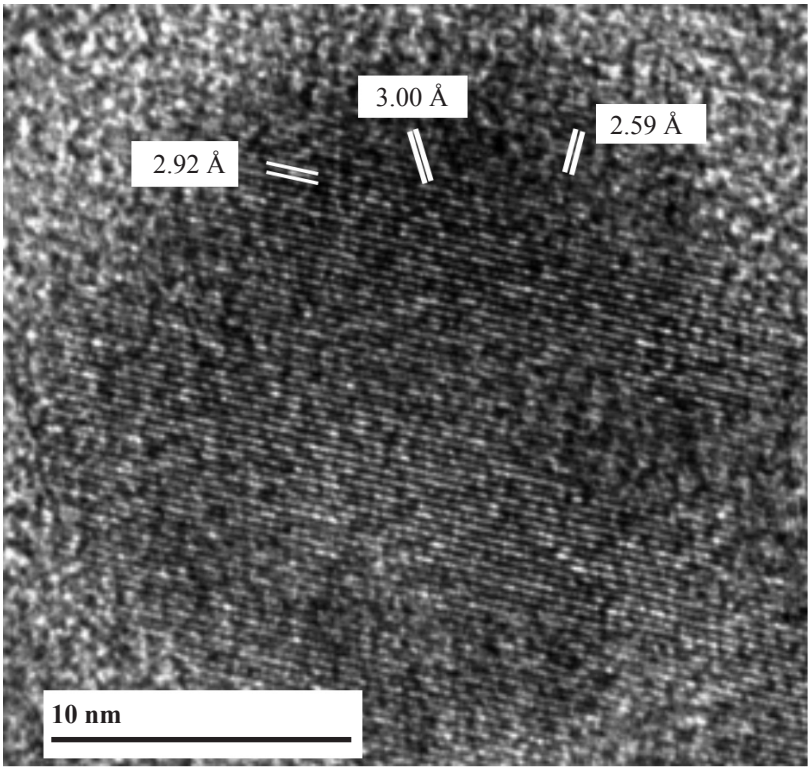

Figure 4. (a) TEM image of IONs with 50 000×, magnification; (b) Histogram of particle size distribution with average size 15.2 nm; (c) TEM image of IONs with 100 000×, magnification and (d) Interplanar distance corresponding to IONs.

properties of the material. As depicted in Figure 5, it confirmed that, IONs are not superparamagnetic because magnetization curve was not intersected at zero point. Superparamagnetic IONs are usually smaller than 20 nm [19]. It is obviously observed as well the presence of hysteresis loop. Hysteresis loop existed because domains of IONs did not return to their original orientation once the applied field was reduced. Maximum estimated single-domain size of magnetite and maghemite are 128 nm and 166 nm [20]. IONs synthesised were single-domain and dependant on particle size. Therefore, coercivity was decreased and could be attributed to small particle size of IONs. Besides, we noticed that IONs achieved 50 emu/g at 1000 G applied magnetic field. This property was useful as its sensitivity allowed magnetic NBR latex to be easily detected by the magnetic detector.

Magnetization curve of NBR and NBR/IONs composites as well as their magnetization saturation, coercivity and remanence are presented in Table 2 and Figure 6, respectively. Coercivity of NBR was increased or reduced from 0 to ±60 G after incorporating IONs into NBR. Besides that, coercivity of NBR/IONs composites had exactly similar coercivity as pure IONs as shown in Figure 4. Remanence on the other hand was increased or reduced from 0 to ±0.22 emu/g after incorporation of IONs into NBR latex. In fact, too high a remanence present in the composite might cause NBR/IONs composite to stick to each other. However, low coercivity and remanence of NBR/IONs composite can be classified as soft magnetic composite materials [21]. Magnetization saturation was increased or reduced from 0 to ±3.8 emu/g when IONs loading was added into NBR

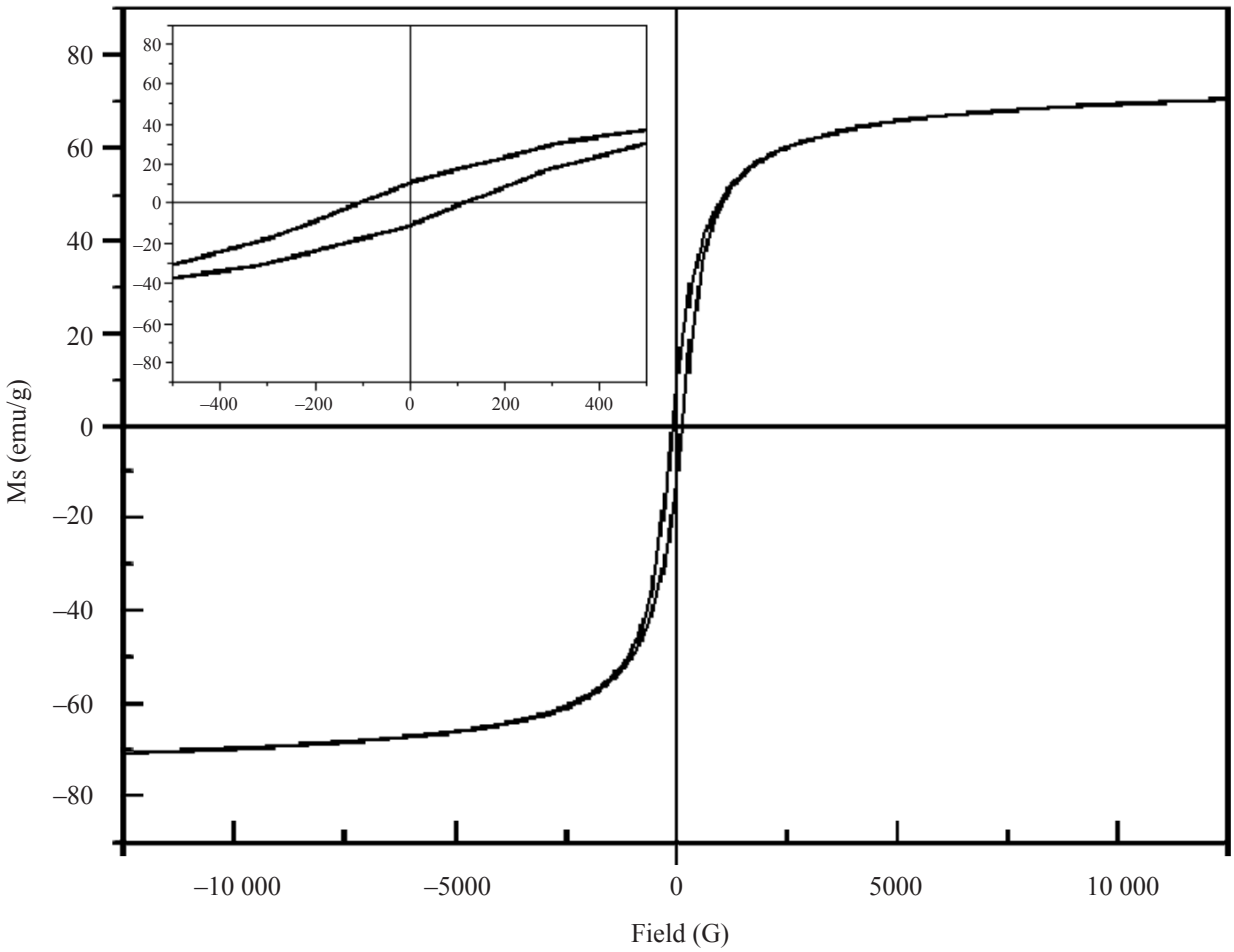

Figure 5. Magnetization curve of IONs.

Table 2. Magnetic properties of NBR latex and NBR/IONs.

	Coercivity, H_c (G)	Remanence, M_r (emu/g)	Magnetization saturation, M_s (emu/g)
NBRlatex	0	0	0
NBR/IONs composite	±60	±0.22	±3.8

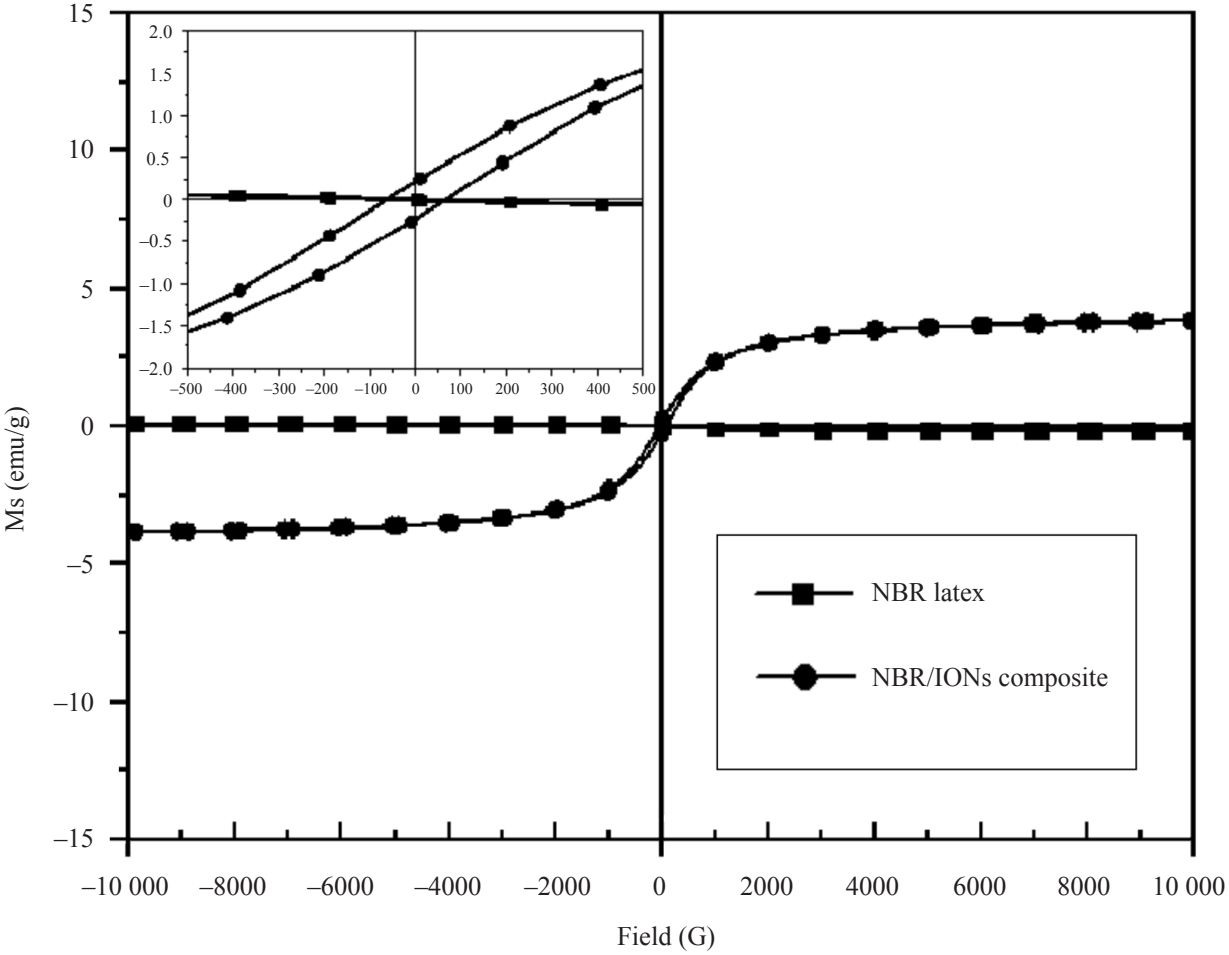

Figure 6. Magnetization curve of NBR latex and NBR/IONs composite.

latex. Magnetization saturation of IONs (70.1 emu/g) was reduced to 3.8 emu/g for NBR/IONs composite attributed to shielding effect of NBR towards IONs and lower concentration of IONs in NBR/IONs composite. According to Marian and Marcin [22], IONs are well align in NBR matrix and it has larger magnetic susceptibility. Therefore, it is suitable to incorporate into NBR latex as proven by NBR/IONs composite that is able to achieve 3.83 emu/g. In our study, a Safeline model S35 metal-particle detector could detect magnetic moment as low as 0.80 emu/g of 10 × 10 mm^2 of latex film composite and NBR/IONs composite has already exceeded the minimum magnetic moment sensor of the detector [23].

CONCLUSION

IONs average size of 15.2 nm was suitable to incorporate with NBR latex films. Zeta potential of IONs was –48.2 mV and stable in pH 9 – 10

medium. This condition was suitable to NBR latex as they had to be prepared in such pH to prevent latex coagulation. Larger crystallite size of IONs proved an increase in magnetic properties. IONs had the most particle size in the range between 18 nm and 20 nm. However IONs tend to agglomerate easily and further studies could be carried out to overcome it. No hematite was observed but only magnetite and maghemite were found, leading to higher magnetization saturation. A high magnetization saturation favoured the sensitivity of magnetic detectors, thus, any torn fragments of NBR/IONs composite film could easily be detected.

ACKNOWLEDGEMENTS

This work was supported by Hartalega Sdn Bhd for a project on nanomagnetic as an additive for nitrile butadiene rubber. The authors would also like to acknowledge the *Fundamental Research Grant Scheme (FRGS: FP049-2013B)* by the Ministry of Higher Education, Malaysia.

REFERENCES

1. Giri, S.K., Pradhan, G.C. and Das, N. (2014) Thermal, electrical and tensile properties of synthesized magnetite/polyurethane nanocomposites using magnetite nanoparticles derived from waste iron ore tailing, *Journal of Polymer Research*, **21** (5), 1–8.
2. Wu, F. *et al*. (2012) Fabrication and characterization of thermo-sensitive magnetic polymer composite nanoparticles, *Journal of Magnetism and Magnetic Materials*, **324** (7), 1326–1330.
3. Vandenberghe, R. *et al*. (2007) *Surface oxidation control of nanosized magnetite and Mössbauer measurements*, in *ICAME 2005*, Springer, pp. 267–271.
4. Nedkov, I. *et al*. (2006) Surface oxidation, size and shape of nano-sized magnetite obtained by co-precipitation, *Journal of Magnetism and Magnetic Materials*, **300** (2), 358–367.
5. Berkowitz, A., Schuele, W. and Flanders, P. (1968) Influence of Crystallite Size on the Magnetic Properties of Acicular γ-Fe_2O_3 Particles, *Journal of Applied Physics*, **39** (2), 1261–1263.
6. Demortiere, A. *et al*. (2011) Size-dependent properties of magnetic iron oxide nanocrystals, *Nanoscale*, **3** (1), 225–232.
7. Kim, D. *et al*. (2001) Synthesis and characterization of surfactant-coated superparamagnetic monodispersed iron oxide nanoparticles, *Journal of Magnetism and Magnetic Materials*, **225** (1), 30–36.
8. Li, Y.-S., Church, J.S. and Woodhead, A.L. (2012) Infrared and Raman spectroscopic studies on iron oxide magnetic nano-particles and their surface modifications, *Journal of Magnetism and Magnetic Materials*, **324** (8), 1543–1550.
9. Slavov, L. *et al*. (2010) Raman spectroscopy investigation of magnetite nanoparticles in ferrofluids, *Journal of Magnetism and Magnetic Materials*, **322** (14), 1904–1911.
10. Harris, L. *et al*., (2003) Magnetite nanoparticle dispersions stabilized with triblock copolymers, *Chemistry of Materials*, **15** (6), 1367–1377.
11. Sun, Y.-P. *et al*. (2006) Characterization of zero-valent iron nanoparticles, *Advances in Colloid and Interface Science*, **120** (1), 47–56.
12. Sun, Y.-P. *et al*. (2007), A method for the preparation of stable dispersion of zero-valent iron nanoparticles, *Colloids and Surfaces A: Physicochemical and Engineering Aspects*, **308** (1), 60–66.
13. Serna, C. *et al*. (2001) Spin frustration in maghemite nanoparticles*, Solid State Communications*, **118** (9), 437–440.
14. Haryono, A., Harmami, S.B. and Sondari, D. (2013) P*reparation of Magnetite Nanoparticles by Thermal Decomposition of Iron (III) Acetylacetonate with Oleic Acid as Capping Agent*, in *Materials Science Forum*, Trans Tech Publ.
15. Eivari, H.A. and Rahdar, A. (2013) Some properties of iron oxide nanoparticles synthesized in different conditions, *World Applied Programming*, **3** (2) 52–55.
16. Martínez-Mera, I. *et al*. (2007), *S*ynthesis of magnetite (Fe< sub> 3</sub> O< sub> 4</sub>) nanoparticles without surfactants at room temperature, *Materials Letters*, **61** (23), 4447–4451.
17. Men, H.-F. *et al*. (2012), Synthesis, properties and application research of atrazine Fe3O4@ SiO_2 magnetic molecularly imprinted polymer,

Environmental Science and Pollution Research, **19** (6), 2271–2280.

18. Zhang, B. *et al*. (2013) *S*uperparamagnetic iron oxide nanoparticles prepared by using an improved polyol method, *Applied Surface Science*, **266**, 375–379.
19. Teja, A.S. and Koh, P.-Y. (2009) Synthesis, properties, and applications of magnetic iron oxide nanoparticles, *Progress in Crystal Growth and Characterization of Materials*, **55** (1), 22–45.
20. Harris, L.A. (2002) *Polymer Stabilized Magnetite Nanoparticles and Poly (Propylene Oxide) Modified Styrene-dimethacrylate Networks*, Ph. D. Thesis, Virginia Polytechnic Institute and State University, Blacksburg, Virginia.
21. Masłowski, M. and Zaborski, M. (2009) *Elastomeric Composites with Magnetorheological and Magnetic Properties Containing Nano-sized Iron Oxide*, Lodz University of Technology Institute of Polymer and Dye Technology, Poland.
22. Zaborski, M. and Masłowski, M. (2011) *Magnetorheological Elastomer Composites*, in *Trends*, in *Colloid and Interface Science XXIV*, Springer.
23. De Ricci, S. and Phalip, P. (1999) *Detectable Polymeric Protective Gloves*, Google Patents.